

COMPREHENSIVE APPROACH TO SYNCHROTRON RADIATION PROTECTION OF NSLS-II

S. Seletskiy[#], T. Shaftan, BNL, Upton, NY 11973, USA

Abstract

To protect the NSLS-II Storage Ring components from possible damage from synchrotron radiation produced by insertion devices (IDs) and bending magnets (BMs) the Active Interlock System (AIS) keeps electron beam orbit within the AI safe envelope (AIE) in the transverse phase space. The NSLS-II beamlines (BLs) and frontends (FEs) are designed under assumption that above certain safe beam current the ID synchrotron radiation (IDSR) fan is produced by the interlocked e-beam. In this paper we describe a new approach to defining the AIS parameters and settings, which significantly simplifies the process of the FE and BL design.

INTRODUCTION

The NSLS-II Storage Ring (SR) [1, 2] includes a number of powerful insertion devices (see [3] for examples) capable of damaging the SR in-vacuum components within 1 ms of exposure time [4].

The active interlock system [5-7] shutting down the electron beam when safe conditions are violated is a necessity for successful operation of NSLS-II synchrotron.

Defining the AIS safe envelope for electron beam for each individual ID is usually a tedious and time-consuming process. Typically it involves several iterations of simulating ID synchrotron radiation distribution on various SR, frontend and ID beamline components, thermal finite element analysis (FEA) and direct raytracing of maximum SR envelope through all respective in-vacuum apertures.

Below we describe a novel approach to this problem based on the back ray-tracing (BRT) and analytic calculation of IDSR power distribution. When algorithmized and programmed, this approach cuts the time spent on finding AIE from weeks to minutes. It also helps to significantly accelerate and simplify the FE design process.

We successfully applied [8] our approach to defining the AIE for a number of IDs recently installed in NSLS-II SR and to designing the respective FEs.

GENERAL IDEA

In our approach we consider each limiting aperture in the SR vacuum chamber that the IDSR fan from individual ID can potentially touch and perform BRT for this aperture. From simple geometric considerations (see Fig. 1) we find respective No-Touch Envelope (NTE) for the electron beam. When e-beam is positioned within the NTE the IDSR fan does not touch the aperture.

Apparently, one must define some reasonable cut-off limits for the tails of the IDSR fan, which will be discussed below.

For the asymmetric horizontal aperture (see Fig. 1) located at distance S from the observation point in vacuum chamber with aperture $\pm A$ the NTE is given by:

$$x' \equiv \alpha_p = \frac{a_p - x}{S}; \quad x' \equiv \alpha_n = -\frac{a_n + x}{S}; \quad x \in [-A, A]$$

To take into account the angular divergence $2\alpha_{div}$ of actual IDSR fan one has to substitute α_p and α_n in this equation with $\alpha_p - \alpha_{div}$ and $\alpha_n + \alpha_{div}$.

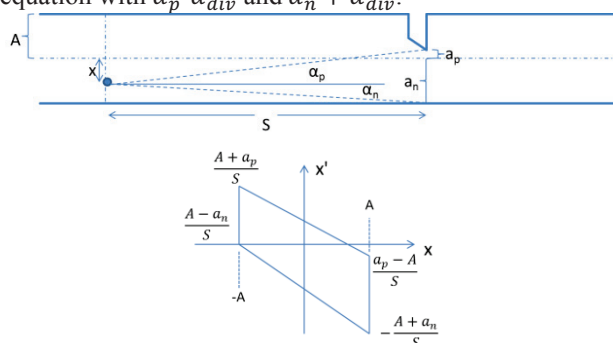


Figure 1: Top plot schematically shows the geometry of limiting horizontal aperture. Bottom plot shows NTE at observation point.

Following the described procedure we define the NTE for each limiting aperture for particular ID and then overlap found NTEs. In case if the ID center does not coincide with the center of the respective straight section we map the obtained NTE to the center of the ID straight. As a result we define the “global” NTE that protects all limiting apertures from IDSR.

POWER DENSITY FROM PLANAR UNDULATOR

To find the power density of IDSR in case of planar undulator or wiggler of arbitrary K we adopt an approach from [9]. The angular power density of the synchrotron radiation from planar undulator with deflection parameter K is:

$$P(\theta, \psi) = \frac{6P_T \gamma^2}{(\pi K)^2} \cdot \int_{b-K}^{b+K} \sqrt{K - (b-y)^2} \frac{a^2 + (2a-4)y^2 + y^4}{(a+y^2)^5} dy$$

$$a = 1 + (\gamma\psi)^2; \quad b = \gamma\theta; \quad P_T = 0.633LI^2B^2; \quad (1)$$

Here L is the undulator length, I is the beam current, E is the beam energy, B is magnetic field of the undulator, γ

#seletskiy@bnl.gov

is relativistic factor and the meaning of angles θ, ψ is shown in Fig. 2

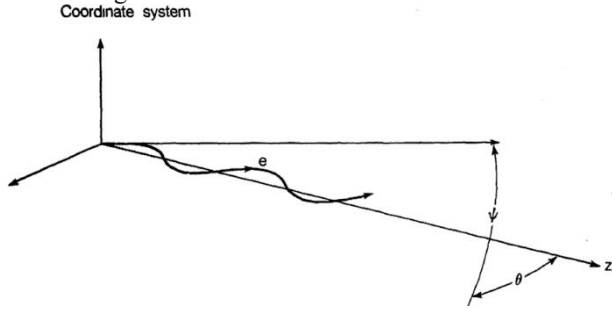


Figure 2: The electron trajectory and coordinate system. The electron moves along the wiggling trajectory in the horizontal plane x - z . θ and ψ are the angles of observation in the horizontal and vertical directions, respectively.

The expression (1) is easy to integrate numerically.

To check validity of obtained results we benchmarked our code with SRW [10]. Comparison of numerical integration of Eq. (1) with SRW calculations shows good agreement of obtained power density distributions down to at least 1 meter distance from observation point to the source of radiation.

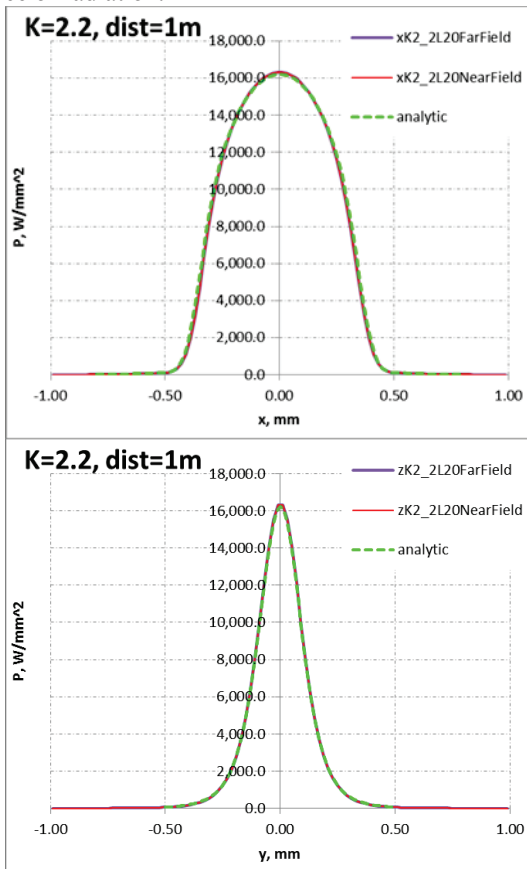


Figure 3: Comparison of numerically integrated Eq. 1 with SRW calculations. Plots show horizontal (upper plot) and vertical (lower plot) power density distribution at 1 m distance from the undulator. Blue and red solid lines give SRW results in far field and near field approximations respectively. Green dotted line shows analytic results.

Plots in Fig. 3 show an example of such comparison performed for one of the proposed NSLS-II IDs (cell 19 LAX ID). LAX ID length is 1 m, its period is 25 mm, its peak magnetic field is 0.94 T and K is 2.2.

We conclude that the precision of analytic formula is quite remarkable. The worst discrepancy that we observed was $\sim 0.5\%$ difference between peak (on-axis) power densities calculated by SRW and from Eq. (1). Such calculation precision is more than enough for the design of IDSR protection.

It is worth to mention that, while analytic estimate assumes “filament” electron beam, in SRW we used exact e-beam parameters. Thus, we conclude that due to the small beam emittance a “single particle” Eq. (1) can be applied to NSLS-II IDs without any farther modifications such as a convolution with realistic beam dimensions.

EXAMPLE OF AIE CALCULATION

Below we will find the AIE for a typical NSLS-II ID.

The typical NSLS-II ID is a 3 m long planar undulator with horizontal polarization centered in the straight section. The vertical divergence of IDSR fan for such devices does not depend on their deflection parameters. For our calculations we choose as a cut-off angle the angle at which power density is 1% of peak on-axis power density of IDSR. This gives ± 0.41 mrad for vertical angular divergence of the fan.

The horizontal divergence of the IDSR fan varies depending on the ID parameters. We choose to perform calculations within ± 1 mrad of horizontal angular divergence. Such value of the collection angle is factor of ~ 2 higher than divergences of any existing or planned NSLS-II IDs ($\sim K/\gamma$) with exception of damping wigglers.

We will perform calculations for the typical ID located in a long straight section, where AIE limits are tighter than these in NSLS-II storage ring short straight section. The horizontal and vertical limiting apertures downstream of an ID in the long straight section can be found in [8].

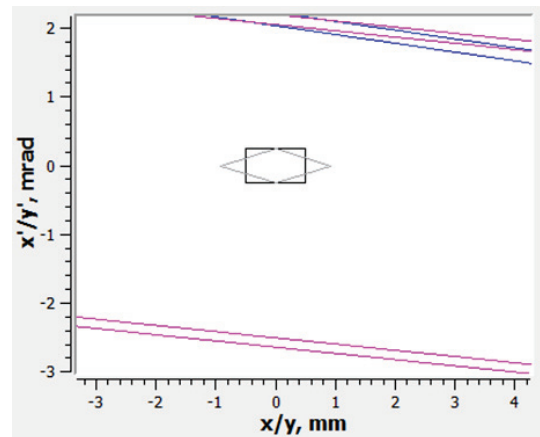


Figure 4: Horizontal BRT for Long straight section. The black rectangle shows ± 0.5 mm, ± 0.25 mrad envelope. Grey diamond shows the respective ± 0.25 mrad envelope and is given for the reference.

We perform the BRT for the described typical ID as discussed in the previous sections. The tracing is done automatically with a dedicated Python-based code.

Figure 4 shows tracing results in horizontal plane for a typical ID in the long straight section.

The NTE is rather large in horizontal direction. It easily accommodates rectangular ± 0.5 mm, ± 0.25 mrad AIE. Of course, one can define much larger horizontal AIE in horizontal plane but this will complicate design of respective FE.

It is worth noticing that from accelerator physics point of view it is reasonable to define the AIE as a diamond shape in the transverse phase space. The ID BPMs are usually located symmetrically on both sides of the center of the straight section. Therefore, interlocking the beam in these IDs within some limits provides the diamond shape interlock at the center of ID straight. On the other hand, our mechanical engineers prefer to use rectangular AI envelope for designing the apertures of respective FE components. Therefore, we, as a rule, define the rectangular AIE for each new ID.

BRT results in long straight section for vertical plane are shown in Fig. 5.

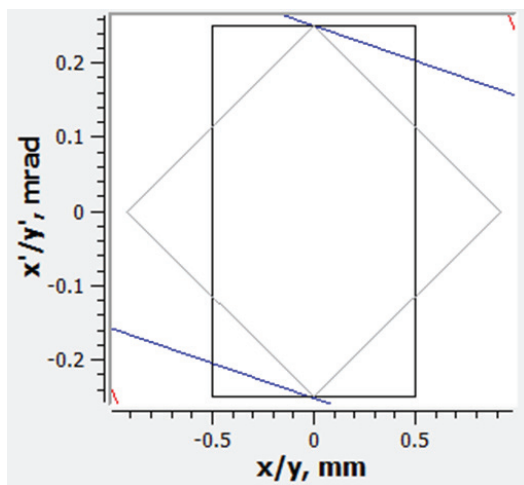


Figure 5: Vertical BRT for the long straight section. Blue lines show borders of dipole chamber NTE. The black rectangle shows ± 0.5 mm, ± 0.25 mrad envelope. Grey diamond shows the respective ± 0.25 mrad envelope and is given for the reference.

The rectangular ± 0.25 mrad, ± 0.5 mm envelope is larger than vertical plane NTE for the long straight section. The e-beam located either at lower left or at upper right corners of such AIE will generate IDSR fan that will be depositing some power on dipole chamber. Thus, FEA was performed for this particular case [11]. It was found that for typical ID the deposited power on the dipole chamber does not cause temperature increase higher than 100 C for angular e-beam deflections of up to 0.5 mrad.

CONCLUSIONS

In this paper we described a novel approach to defining the synchrotron radiation protection envelope for electron beam in the storage rings.

We demonstrated application of our approach to defining safe active interlock envelope for a typical insertion device installed in the long straight section of the NSLS-II storage ring.

This approach is based on the back ray tracing and analytic calculation of insertion device synchrotron radiation power distribution.

We algorithmized and programmed described approach in a dedicated Python-based code.

We successfully applied the devised algorithm to defining safe active interlock envelopes for a number of insertion devices recently installed in NSLS-II storage ring.

By utilizing the described approach we tremendously facilitated the analysis of safety considerations for insertion device operation. We also significantly accelerated and simplified the process of new frontends design.

ACKNOWLEDGEMENTS

We are grateful for support from the NSLS-II. This work is supported in part by the U.S. Department of Energy (DOE) under contract No. DE-AC02-98CH1-886.

REFERENCES

- [1] F. Willeke, "Commissioning Results of NSLS-II", IPAC'15, Richmond, Virginia, USA, 2015.
- [2] T. Shaftan, "A Matlab Interface Package for Elegant Simulation Code", IPAC'16, Busan, Korea, 2016, WEPOY054, this conference.
- [3] A. Broadbent et al., "RSI for the Front-Ends for the Six NSLS-II Project Beamlines", LT-C-XFD-RSI 1.04.06, 2010.
- [4] P. Ilinski, V. Ravindranath, O. Tchubar, "Maximum Response Time of NSLS-II Active Interlock Equipment Protection System", 2011.
- [5] J. Choi, F. Willeke, NIM A 681 (2012) 1-6.
- [6] S. Seletskiy et al., "Commissioning of Active Interlock System for NSLS II Storage Ring", TUPMA057, IPAC'15, Richmond, Virginia, USA, 2015.
- [7] S. Seletskiy et al., THU-P-084, Proceedings of SRI2016, 2015.
- [8] S. Seletskiy, T. Shaftan, BNL-108464-2015-IR, 2015.
- [9] K. J. Kim, NIM A 246 (1986) 67-70.
- [10] O. Chubar, P. Elleaume, "Accurate and Efficient Computation of Synchrotron Radiation in the Near Field Region", EPAC'98, Stockholm, Sweden, 1998.
- [11] V. Ravindranath, "Dipole Chamber FEA-Active interlock envelope for IVU beam", 4/26/2011.